Journal of Cell Science 111, 3059-3071 (1998)
Printed in Great Britain © The Company of Biologists Limited 1998
JCS4602

The IQGAP-related protein DGAP1 interacts with Rac and is involved in the modulation of the F-actin cytoskeleton and control of cell motility

Jan Faix[1,*], Chris Clougherty[1], Angelika Konzok[1], Ursula Mintert[1], John Murphy[1], Richard Albrecht[1], Bettina Mühlbauer[1] and Jürgen Kuhlmann[2]

[1]Max-Planck-Institut für Biochemie, D-82152 Martinsried, Germany
[2]Max-Planck-Institut für molekulare Physiologie, D-44026 Dortmund, Germany
*Author for correspondence (e-mail: faix@biochem.mpg.de)

Accepted 8 August; published on WWW 23 September 1998

SUMMARY

DGAP1 of *Dictyostelium discoideum* is a cell cortex associated 95 kDa protein that shows homology to both RasGTPase-activating proteins (RasGAPs) and RasGAP-related proteins. When tested for RasGAP activity, recombinant DGAP1 protein did not promote the GTPase activity of human H-Ras or of *Dictyostelium* RasG in vitro. Instead, DGAP1 bound to *Dictyostelium* Rac1A and human Rac1, but not to human Cdc42. DGAP1 preferentially interacted with the activated GTP-bound forms of Rac1 and Rac1A, but did not affect the GTPase activities. Since Rho-type GTPases are implicated in the formation of specific F-actin structures and in the control of cell morphology, the microfilament system of mutants that either lack or overexpress DGAP1 has been analysed. DGAP1-null mutants showed elevated levels of F-actin that was organised in large leading edges, membrane ruffles or numerous large filopods. Expression of actin fused to green fluorescent protein (GFP) was used to monitor the actin dynamics in these cells, and revealed that the F-actin cytoskeleton of DGAP1-null cells was rapidly re-arranged to form ruffles and filopods. Conversely, in DGAP1-overexpressing cells, the formation of cellular projections containing F-actin was largely suppressed. Measurement of cell migration demonstrated that DGAP1 expression is inversely correlated with the speed of cell motility.

Key words: Actin cytoskeleton, Cell motility, *Dictyostelium*, IQGAP, Rac

INTRODUCTION

The actin cytoskeleton is involved in cell adhesion and motility, mitogenesis, cytokinesis, and establishment of morphology (Ridley and Hall, 1992; Stossel, 1993; Larochelle et al., 1996; Braga et al., 1997). The Ras-related members of the Rho family of small GTP-binding proteins are key regulators of cytoskeletal organisation. These proteins operate as binary molecular switches by cycling between the active GTP-bound state and the inactive GDP-bound state (Boguski and McCormick, 1993). In Swiss 3T3 fibroblasts, the activated forms of Cdc42, Rac, and Rho are implicated in the formation of distinct F-actin structures. Activated Cdc42 induces the formation of microspikes and filopodia, activated Rac leads to the formation of membrane ruffles or lamellipodia, and activated Rho induces the formation of stress fibers linked to focal adhesions plaques (Ridley and Hall, 1992; Ridley et al., 1992; Nobes and Hall, 1995).

In addition to these unique types of reactions, biochemical and genetic evidence revealed that these GTPases are co-ordinated to form a linear, hierarchical cascade (Nobes and Hall, 1995; Chant and Stowers, 1995). Activation of Cdc42 leads to the stimulation of Rac activity, which in turn promotes the activation of Rho (Kozma et al., 1995; Nobes and Hall, 1995). Whereas the upstream events leading to activation of these GTPases are well understood, less is known about the molecular events down-stream of GTPase activation which lead to modulation of the actin cytoskeleton. Some candidate effector proteins for the Rho-family GTPases have already been reported. Activated Rho interacts with target molecules such as Rho kinase (Matsui et al., 1996), myosin phosphatase (Kimura et al., 1996), and protein kinase N (Amano et al., 1996), indicating that Rho acts on the cytoskeleton through the acto-myosin system. Additional targets of activated Rho have been reviewed by Van Aelst and D'Souza (1997).

The target proteins of activated Cdc42 and Rac1 have been identified as POR1 (Van Aelst et al., 1996), p67phox (Diekmann et al., 1994), PI3-kinase (Zheng et al., 1994), phosphatidylinositol 4-phosphate 5-kinase (Hartwig et al., 1995), ACK (Manser et al., 1993), PAK (Manser et al., 1995; Martin et al., 1995), WASP (Symons et al., 1996), and IQGAP1 and IQGAP2 (Hart et al., 1996; Brill et al., 1996; McCallum et al., 1996; Kuroda et al., 1996). The C-terminal halves of the IQGAPs show considerable homology to the catalytic domains of RasGTPase-activating proteins, and bind with these domains preferentially to the activated forms of Cdc42 and Rac1, but not to GTP or GDP-bound of forms Rho and Ras (Hart et al., 1996; Brill et al., 1996). The N-termini of IQGAP1 and

IQGAP2 harbor multiple protein-protein interaction motifs such as the IQ-repeats responsible for binding of IQGAPs to calmodulin (Weissbach et al., 1994; Hart et al., 1996; Brill et al., 1996), and a calponin homology domain that is found in the actin-binding sites of F-actin binding proteins (Djinovic Carugo et al., 1997). IQGAP1 was also shown to directly bind and cross-link F-actin filaments (Bashour et al., 1997).

Previously we have reported on the discovery of DGAP1 of *D. discoideum* from acto-myosin complexes (Faix and Dittrich, 1996; Faix et al., 1996). This protein shows sequence similarities to RasGTPase-activating proteins (RasGAPs) and RasGAP-related proteins, in particular to the C-terminal halves of human IQGAP1 and IQGAP2 (Weissbach et al., 1994; Brill et al., 1996), and to full length yeast Sar1/Gap1 (Imai et al., 1991; Wang et al., 1991). The recently identified GAPA from *D. discoideum* is most closely related to DGAP1 (Adachi et al., 1997). *D. discoideum* mutants have been established that either lack or overexpress DGAP1 protein 3-fold. Elimination of DGAP1 by gene replacement resulted in substantially larger colonies of *D. discoideum* cells on bacterial lawns and in the formation of multi-tipped fruiting bodies during development, whereas overexpression of DGAP1 lead to a defect in cytokinesis. The null and overexpressing mutants indicated that DGAP1 is involved in the control of cytoskeletal activities in *D. discoideum*.

In the present study we demonstrate that DGAP1 lacks RasGAP activity in vitro and that it preferentially interacts with activated forms of human Rac1 and *D. discoideum* Rac1A. Our results indicate that DGAP1 of *D. discoideum* is a structural and functional homologue of mammalian IQGAPs. We present a functional link between Rac1A, DGAP1, and modulation of the microfilament system, in particular the polymerisation of actin. Motility of growth-phase cells is increased in DGAP1-null mutants and decreased in transformants that overexpress DGAP1.

MATERIALS AND METHODS

Protein expression and purification

For expression of His-tagged DGAP1, cDNA fagments coding for residues 1-882, 161-822, 161-644, and 644-822 of DGAP1 were generated by PCR using primers designed to obtain a *Bam*HI site at the 5′ end and a *Pst*I site at the 3′ end. The amplified products were cloned into expression vector pQE32 (Qiagen), the sequences verified, and the His-tagged DGAP1 constructs were expressed in *Escherichia coli* host M15. The recombinant proteins were purified from the soluble fraction of bacterial extracts on Ni^{2+}-NTA-agarose (Qiagen) as recommended by the manufacturer.

Human H-Ras, Cdc42Hs and Rac1, and *D. discoideum* Rac1A, RacC, RacE, and RasG and the two DGAP1 constructs encoding residues 1-822 and 161-822 were expressed as GST (glutathione S-transferase)-fusion proteins in *E. coli* strain JM83 using pGEX vectors (Pharmacia), and purified according to the instructions of the manufacturer. After purification all GST-fusion proteins were dialysed against PBS containing 140 mM NaCl, 2.7 mM KCl, 10 mM Na_2HPO_4, pH 7.3, supplemented with 1 mM $MgCl_2$, 1 mM benzamidine, 2 mM DTT, and 0.1% NaN_3. GST-Cdc42 and GST-H-Ras were expressed according to the method of Ahmadian et al. (1997a) and Lenzen et al. (1998), the GST-construct for expression of Rac1 was a gift from Dr R. Cool, and the GST-RacE construct was kindly provided by Dr A. De Lozanne. *D. discoideum* Rac1A, RacC, and RasG were amplified from a λgt11 cDNA library (Clonetech), the sequences verified, and cloned into suitable restriction sites of pGEX vectors.

Synthesis and purification of p21 H-Ras was essentially performed as described (Tucker et al., 1986). GAP-334 (the catalytic domain from human p120GAP, residues 714-1047) was expressed and purified according to the method of Scheffzek et al. (1997a). The purified catalytic domain of human p50RhoGAP (Lancaster et al., 1994), spanning amino-acid residues 189-439, was kindly provided by Dr R. Mittal.

RasGAP and RhoGAP assays

To assay RasGAP activity purified Ras proteins were converted to their GTP-bound form by incubation of protein solutions with a 50-fold excess of GTP in the presence of 40 mM EDTA and 200 mM $(NH_4)_2SO_4$ at 0°C according to the method of John et al. (1990). After 1 hour, the reaction mixture was applied to a HiTrap™ desalting column (Pharmacia), which was equilibrated with 20 mM Tris-HCl, pH 7.5, 5 mM $MgCl_2$, 1 mM DTE. Elution of the mixture with the equilibration buffer resulted in separation of protein and free nucleotide. Fractions were analysed by Bradford assay for protein concentration. Nucleotide concentrations were analysed by C18 reversed phase HPLC (ODS Hypersil, 5 μm, Bischoff) on a Beckman HPLC (System Gold) using 100 mM K-phosphate, pH 6.5, 10 mM tetrabutyl-ammonium-bromide, 0.2 mM NaN_3 and 7.5% acetonitrile as the mobile buffer phase.

To measure the effect of DGAP1-constructs on GTP-hydrolysis by Ras proteins, Ras*GTP was incubated with the putative GTPase-activating protein to the final concentration as indicated for 1 hour at 25°C in 20 mM Tris-HCl, pH 7.5, 5 mM $MgCl_2$, 1 mM DTE. To prevent further GTP-hydrolysis, samples were snap-frozen in liquid nitrogen and thawed directly before analysis. The catalytic domain of p120RasGAP (GAP-334) was used as a positive control. Intrinsic and stimulated GTP-hydrolysis was monitored with HPLC as described above. To determine the effect of DGAP1 on GTP-hydrolysis by Rac proteins, either 20 μM Rac1*GDP or 20 μM Rac1A*GDP were incubated with 1, 2, 4, or 10 μM of His-DGAP1(161-822) fusion protein for the time points indicated at 37°C in 20 mM Tris-HCl, pH 7.5, 5 mM $MgCl_2$, 1 mM DTE. The catalytic domain of p50RhoGAP or bovine serum albumin (BSA) were used as controls. Concentrations of GTP were monitored as described.

GST-fusion protein binding assays

For binding assays, purified GST-fusion protein were bound to GST agarose beads and converted to their GDP or GTP-bound form by incubation of 500 μg of each protein for 1 hour at 4°C with a 10-fold molar excess GDP or GTPγS in the presence of 5 mM EDTA and 5 mM $(NH_4)_2SO_4$ in PBS-buffer. The reaction was stopped by the addition of $MgCl_2$ to a final concentration of 10 mM. For the binding experiments the beads were incubated with 1 ml each with lysate (approximately 2 mg protein/ml) prepared from AX2 growth-phase cells with lysis buffer containing 25 mM Tris-HCl; pH 7.4, 50 mM NaCl, 5 mM $MgCl_2$, 2 mM EGTA, 2 mM DTT, 1% *n*-octylpolyoxyethylene (Bachem), 2 mM benzamidine, bestatin (0.5 μg/ml), and pepstatin, antipain, and leupeptin (each 1 μg/ml). After 1 hour of incubation at 4°C, the beads were sedimented, washed five times with 1 ml lysis buffer, and bound proteins eluted with SDS sample buffer. DGAP1 interaction was determined in western blots using anti-DGAP1 antibody 216-394-1.

Culture conditions and transformation of *D. discoideum* cells

Cells of the AX2 wild-type strain and of DGAP1-mutants transformants were cultivated at 23°C axenically in nutrient medium (Watts and Ashworth, 1970) as specified by Claviez et al. (1982). Cells of DGAP1-null mutant G10– (Faix and Dittrich, 1996) were transformed by calcium phosphate-mediated transformation (Nellen et al., 1984) with a vector for expression of a red-shifted, S65T, GFP-

actin fusion protein as previously described (Westphal et al., 1997). Transformants were selected on plates with 20 μg/ml G418 (Difco) and cloned by spreader dilutions on *Klebsiella aerogenes*. Independent transformants that expressed GFP-actin were isolated. Since they showed the same phenotype, the clonal cell line HG1690, here referred to as G10-GFPA was chosen and used for all experiments. The transformant HG1662, here referred to as AX2GFPA, which was previously obtained after transformation of AX2 wild-type cells with the same construct was used as a control (Westphal et al., 1997).

Monoclonal antibodies, immunoblotting, quantification of F-actin and microscopy

Proteins were resolved by SDS-PAGE in 10% gels, and immunoblotting was performed by standard procedures using anti-DGAP1 antibody mAb 216-394-1 culture supernatant (Faix and Dittrich, 1996), anti-GST-antibody mAb mAb 268-44-6 culture supernatant (this paper) and ^{125}I sheep anti-mouse IgG (Amersham). For quantification of proteins, western blots were incubated with iodinated anti-actin antibody mAb 224-236-1 (Westphal et al., 1997) and anti-α-actinin antibody mAb 47-18-9 (Schleicher et al., 1988). The antibody ^{125}I-labelled bands were analysed with a Fuji Phosphoimager and the PCBAS program.

For immunofluorescence labelling, growth-phase cells were washed twice with 17 mM Na/K-phosphate buffer, pH 6.0, and allowed to adhere on glass coverslips for 20 minutes. The cells were then fixed with picric acid/paraformaldehyde (Humbel and Biegelmann, 1992), and labelled for F-actin with 0.5 μg/ml of TRITC-conjugated phalloidin (Sigma).

For the calculation of fluorescence intensity distribution of TRITC-phalloidin labelled cells, confocal sections were obtained using a Zeiss LSM 410 inverted microscope (Zeiss) equipped with ×40 Plan-NEOFLUAR objective. From these images pixel intensities were extracted along an adjustable line that crosses the cell. For averaging intensity distributions, background was substracted, and line scans from 50 cells were normalised with respect to the cell diameter.

For quantification of actin cells were harvested during the exponential growth, washed twice with 17 mM Na-K-phosphate buffer, pH 6.0, and 2×10^7 cells allowed to attach to 10 cm plastic Petri dishes for 20 minutes at room temperature. Subsequently the Na-K-phosphate buffer was removed and the cell lysed with 10 ml ice-cold buffer containing 80 mM Pipes, pH 6.8, 5 mM EGTA, 30% glycerol, 5 mM $MgCl_2$, 1 mM DTT, 1% Triton X-100, and protease inhibitors as described. The actin concentration in the lysates was approximately 0.3 μM. 200 μl samples were spun for 40 minutes at 4°C at 27 psi in a Beckman airfuge (Beckman), and the pellets and supernatants were resuspended to equal volumes in SDS sample buffer. Total proteins in pellet and supernatant fractions were separated with SDS-PAGE, blotted to nitrocellulose, incubated with iodinated anti-actin antibody mAb 224-236-1 (Westphal et al., 1997), and actin quantified as described. High speed co-sedimentation assays of full-length His-DGAP1(1-822) with F-actin were performed essentially as described (Faix et al., 1996).

For double view microscopy of living cells expressing GFP-actin fusions, the cells were harvested from nutrient medium, washed twice in 17 mM Na-K-phosphate buffer, pH 6.0, and monitored moving on glass with an inverted Zeiss Axiovert 100 fluorescence microscope that was equipped with an additional dichroic mirror (580 nm, Zeiss) near the two video outputs of the microscope for the simultaneous observation of fluorescence and phase contrast images. The phase contrast was recorded with red light (Cy5 excitation filter; HQ 620/60; GFP (AHF). The green and blue wavelengths were used in connection with the standard filter set Endow-GFP (AHF) for monitoring GFP-fluorescence. Aquisition of GFP and phase contrast images were performed with synchronised SIT C2400-08 (Hamamatsu) and CCD XC-75CE (Sony) video cameras. With an adapted PC based colour frame grabber (MVC-Image Capture PCI, Imaging Technology Inc.) dual images were stored on the hard disk.

Determination of generation times, phagocytosis and motility assays

Generation times of cells were determined by plating single cells together with a suspension of *Klebsiella aerogenes* on SM nutrient agar plates. The cells were monitored with an inverted Axiovert 35 microscope (Zeiss) equipped with a 10× ACHROPLAN objective and a CCD camera coupled to a Panasonic 6720 time lapse recorder (Matsushita Electric). The generation time was expressed as the time interval between two mitotic cell divisions.

To quantify phagocytosis, the uptake of TRITC-labelled yeast particles was determined as described (Maniak et al., 1995). To account for differences in the cell volumes of the cell lines, the volume of densely packed cells was measured by centrifugation of cells into a graded glass tube (Gerisch, 1960). For the phagocytosis assay, the total volume of wild-type and mutant cells was adjusted to 2 μl of densely packed cells per ml, which corresponds to 2×10^6/ml of wild-type cells. Total protein content was verified in immunoblots with anti-actin antibodies as described.

Quantitative analysis of cell motility of growth-phase cells using a Zeiss IM 35 inverted microscope and image-processing system was essentially performed according to the method of Segall et al. (1987) and Fisher et al. (1989), except that instead of using a chemotaxis chamber, migration of cells was analysed in nutrient medium on 5 cm × 5 cm BSA-coated (10 mg/ml) glass coverslips. For each experiment a field containing approximately 100 cells was monitored, and data were collected every 45 seconds at intervals for a 30 minutes period.

RESULTS

DGAP1 possesses no in vitro RasGAP activity but preferentially interacts with activated Rac

In order to examine whether DGAP1 acts as a RasGAP, we expressed full length (residues 1-822) and truncated DGAP1 (residues 161-644) as glutathione S transferase (GST)-fusion proteins in *E. coli* and assayed these proteins for RasGAP activity with recombinant human H-Ras charged with GTP. However, neither truncated DGAP1, containing the GAP-related domain, nor full length DGAP1 stimulated the GTPase of H-Ras, whereas the catalytic fragment of human p120RasGAP (GAP-334) strongly activated GTP hydrolysis of H-Ras (Fig. 1A). Since it was conceivable that DGAP1 acts as a RasGAP, but can stimulate GTP hydrolysis only with *D. discoideum* Ras proteins, we repeated the GTPase assay with RasG, a Ras protein that is maximally expressed during growth and early development of *D. discoideum* cells (Robbins et al., 1992; Khosla et al., 1996). GAP-334 stimulated the GTPase activity of *D. discoideum* RasG, but no GAP activity was detected for both truncated and full-length DGAP1 (Fig. 1B). From these results we conclude that DGAP1 lacks in vitro RasGAP activity.

Considering the significant sequence homology of DGAP1 to the C-termini of human IQGAPs we investigated whether DGAP1 interacts with human H-Ras, Cdc42Hs, and Rac1. In order to test this we performed in vitro binding experiments with H-Ras, Cdc42Hs and Rac1 that have been expressed as GST-fusion protein in *E. coli*. The glutathione Sepharose-bound GTPases were loaded with either GDP or GTPγS (guanosine 5′-O-(3-thio)triphosphate), and incubated with lysates prepared from AX2 wild-type cells. After repeated

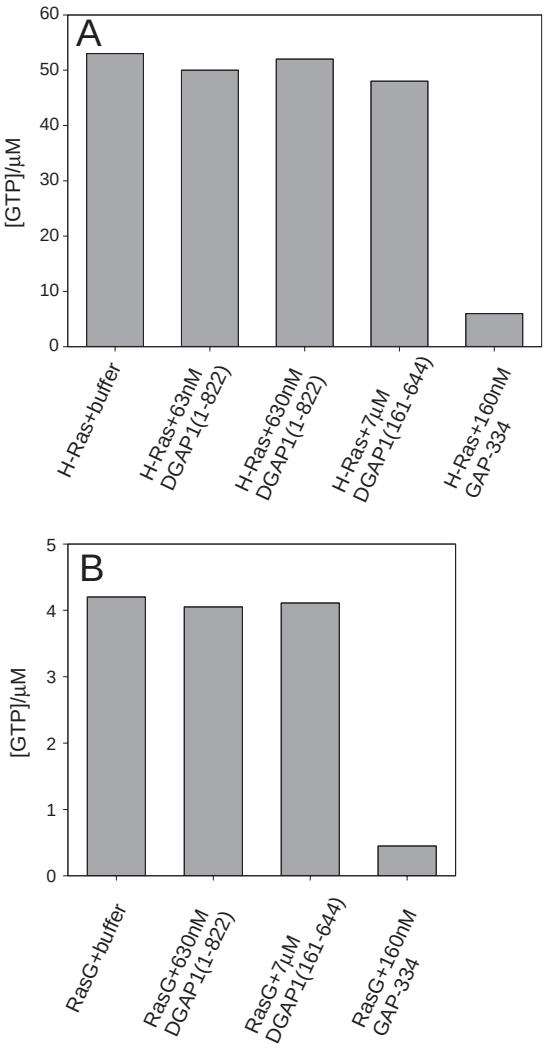

Fig. 1. DGAP1 lacks in vitro RasGAP activity. The results of the in vitro RasGAP assays are shown as the concentration of GTP bound to human H-Ras (A) or *Dictyostelium* RasG (B) after a 1 hour incubation at 25°C with full length DGAP1 (residues 1-822) or with truncated DGAP1 (residues 161-644), containing the GAP-related domain. Neither 7 µM of truncated DGAP1 nor 63 nM or 630 nM of full length DGAP1 stimulated the GTPase of H-Ras, whereas already 160 nM of the catalytic fragment of human p120RasGAP (GAP-334) strongly activated GTP hydrolysis of H-Ras. Similar results were obtained for RasG. GTP concentrations were determined by reverse phase HPLC.

washing of the beads, the presence of bound DGAP1 was analysed by western blotting with DGAP1-specific monoclonal antibody mAb 216-394-1 (Faix and Dittrich, 1996). As shown in Fig. 2A, DGAP1 bound strongly to Rac1, but not to H-Ras, Cdc42Hs or to the GST control. The association of DGAP1 with Rac1 was most prominent when GTPγS was bound to the GTPase, indicating that DGAP1 binds preferentially to the activated, GTP-bound form of Rac1. After prolonged exposure of the film, DGAP1 interaction was also seen with Rac1*GDP.

Next, we tested DGAP1 interaction with small GTPases from *D. discoideum*. Since neither a Cdc42 nor a Rho homologue have been discovered in *D. discoideum* thus far, we performed similar binding experiments with three Rac proteins of the eight Racs that have been described for *D. discoideum* (Bush et al., 1993; Larochelle et al., 1996): Rac1A, a Rac protein that shows more than 85% identity to human Rac1 (Bush et al., 1993), RacE, a protein involved in the control of cytokinesis (Larochelle et al., 1996), and RacC that is 61% identical to Rac1. Due to the considerable sequence relationship of DGAP1 to the catalytic domain of RasGAPs, we also tested whether RasG has the capacity to bind to DGAP1. As shown in Fig. 2B, strong binding of DGAP1 was observed for both RacE and Rac1A. However, the guanine nucleotide dependent binding of DGAP1 was only seen for Rac1A. Compared with Rac1A, a very weak interaction was seen for RasG and for RacC, and no binding was detected for the GST-control. Taken together, these experiments suggest that DGAP1 interacts with a subset of Rac proteins that are present in *D. discoideum* and that activated Rac1A is a predominant target of DGAP1.

DGAP1 interacts directly with Rac1A

DGAP1 does not possess a CRIB motif, which has been implicated in binding of PAK and other target proteins to Cdc42/Rac GTPases (Burbelo et al., 1995). To identify the binding domain of DGAP1 to Rac1A, full-length (residues 1-822) and truncated forms (residues 161-644, 161-822, and 644-822) of DGAP1 were expressed and purified as N-terminal His-tagged fusion proteins from *E. coli*, and their direct interactions with Rac1A were examined in binding experiments similar to those described above. As depicted in Fig. 2C, His-DGAP1(1-822) and His-DGAP1(161-822) bound strongly and preferentially to the activated form Rac1A, whereas His-DGAP1(161-644) and His-DGAP1(644-822) either did not bind or bound with an affinity too low to be detected in this assay. From these experiments, we conclude first that DGAP1 interacts directly with Rac1A and second, that residues 161-822 of DGAP1, containing the GAP-related domain in conjunction with the C terminus, are required for high affinity binding to activated Rac1A.

DGAP1 does not influence the intrinsic RacGAP activity

To determine whether DGAP1 affects the GTPase activities of Rac proteins, we first tried to measure RacGAP activity in experiments similar to the RasGAP assay. However, the rapid intrinsic GTP hydrolysis rates of both, human Rac1 and *D. discoideum* Rac1A, precluded the isolation of sufficient quantities of Rac1 or Rac1A in their GTP-bound forms. Thus, 20 µM Rac1*GDP or 20 µM Rac1A*GDP were incubated in the presence of a tenfold excess of free GTP. Due to the fast and spontaneous nucleotide exchange reactions, both Racs bound free GTP-nucleotides from the solution, that in turn were hydrolysed to GDP. Monitoring the intrinsic GTP hydrolysis rates of Rac1 or Rac1A was possible at 37°C, since at this temperature the nucleotide exchange reactions of both GTPases were faster than the rate limiting step of GTP hydrolysis. The GTP hydrolysis by *D. discoideum* Rac1A was approximately 50% faster than that of human Rac1 in this assay (Fig. 3A,B). Addition of 1 µM of the catalytic domain of p50RhoGap increased Rac-mediated GTP hydrolysis rates of both GTPases, whereas the addition of 1 µM of His-DGAP1(161-822) resulted in GTP hydrolysis rates that were

similar to the buffer controls, indicating that DGAP1 does not affect the intrinsic GTPase activities of the tested Rac proteins. To confirm this assumption, Rac1A*GDP was incubated for 45 minutes with 100 μM GTP in the presence of varying concentrations of His-DGAP1(161-822) or BSA and p50RhoGap as control proteins (Fig. 3C). Increasing amounts of DGAP1 appeared to slightly inhibit Rac1A-mediated GTP hydrolysis. However, these values were in the range of the buffer and BSA controls, whereas 1 μM of the catalytic domain of p50RhoGAP clearly stimulated the GTPase of Rac1A. From these results we conclude that DGAP1 has in vitro neither RacGAP activity nor does it affect the intrinsic GTPase activity of Rac1A.

Altered cell shape and organisation of F-actin in DGAP1-mutants

To determine the influence of DGAP1 protein on cell shape and organisation of F-actin, we employed phase contrast and fluorescence microscopy of TRITC-phalloidin labelled cells to compare the DGAP1-null mutant G10– and the DGAP1 overexpressing transformant G2++ with wild-type AX2 cells (Fig. 4). In AX2 cells, F-actin was found to be enriched in the

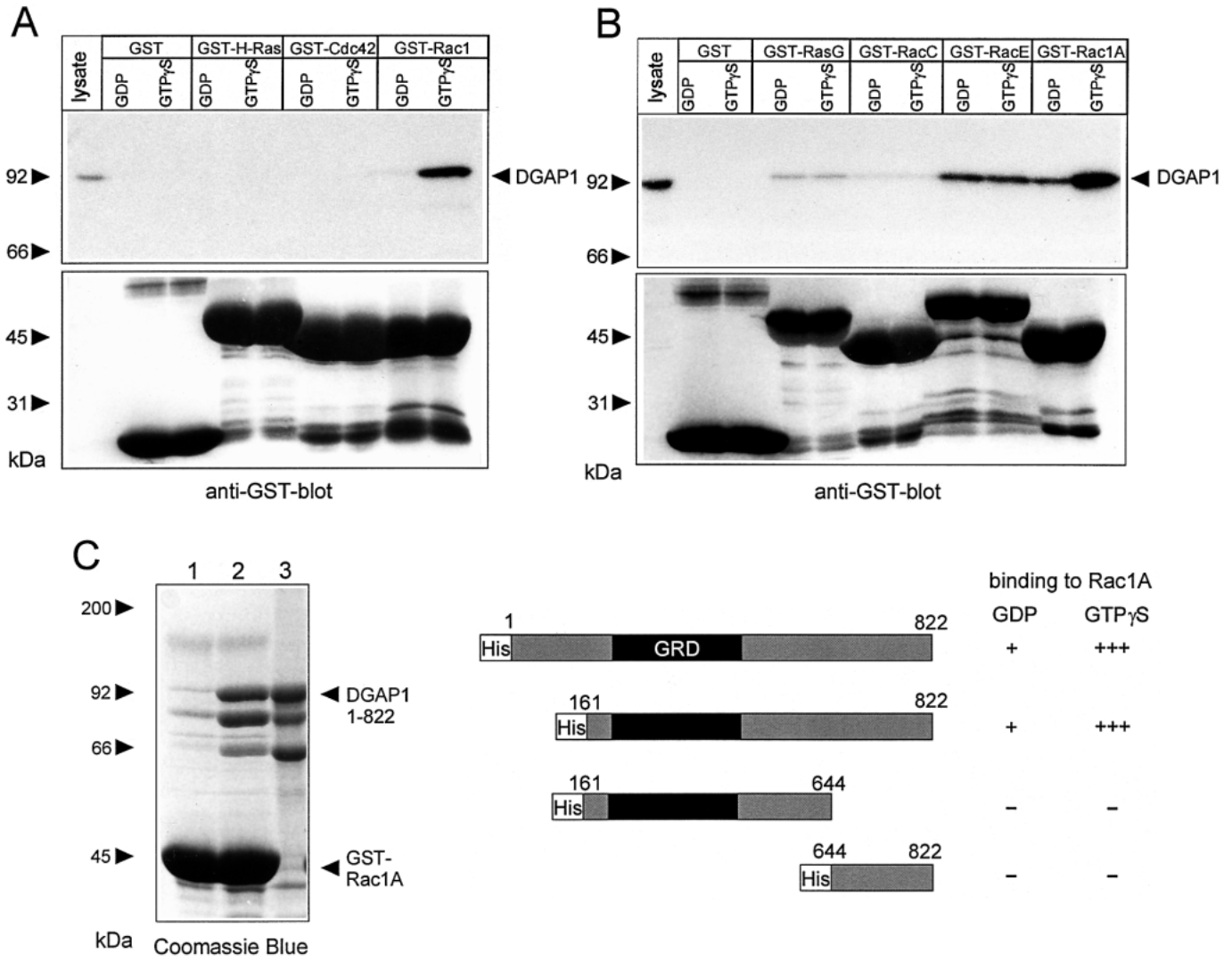

Fig. 2. DGAP1 binds to Rac GTPases. (A,B) The glutathione-sepharose bound GST-fusion proteins indicated were charged with either GDP or GTPγS and were incubated for 1 hour with lysates prepared from AX2 wild-type cells. Proteins remaining on the washed beads were eluted with 200 μl SDS sample buffer, and 10 μl aliquots subjected to SDS-PAGE. After blotting onto nitrocellulose, DGAP1 interaction was detected in immunoblots with anti-DGAP1 antibody mAb 216-394-1 followed by ^{125}I anti-mouse IgG labelling. Parallel blots were labelled with anti-GST-antibody mAb 268-44-6 followed by ^{125}I anti-mouse IgG labelling to demonstrate that comparable amounts of the corresponding GST-fusion protein were used in these assays. (C) Binding experiments with recombinant DGAP1 constructs and *Dictyostelium* Rac1A. Full-length or truncated forms of DGAP1 indicated have been expressed and purified as N-terminally His-tagged fusion protein in *E. coli* and tested for interaction with GST-Rac1A as described. The strong binding of activated Rac1A to full-length DGAP1 demonstrates that this interaction is direct and not mediated by other proteins (left). Lane 1: GST-Rac1A*GDP and His-DGAP1(1-822); lane 2: GST-Rac1A*GTPγS and His-DGAP1(1-822); lane 3: His-DGAP1(1-822) control. The two bands below full-length DGAP1 are degradation products of DGAP1, that retained the ability to interact with activated Rac1A. Mapping of the DGAP1-binding site to Rac1A (right). The GAP-related domain (GRD) is highlighted in black.

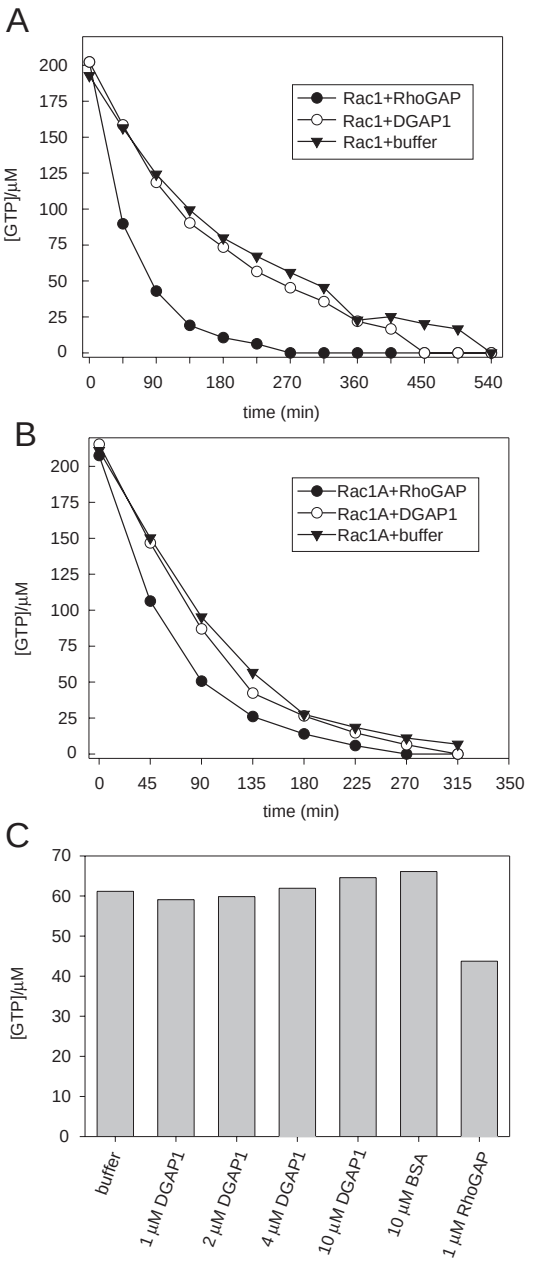

Fig. 3. DGAP1 does not affect the intrinsic GTPase activities of human Rac1 or of *D. discoideum* Rac1A. (A,B) GTPase activities of 20 µM Rac1*GDP or 20 µM Rac1A*GDP in the presence of 200 µM free GTP were determined by incubation with either 1 µM His-DGAP1(161-822), 1 µM p50RhoGAP or incubation buffer alone. (C) GTP hydrolysis rates of 20 µM Rac1A*GDP in the presence of increasing amounts (1, 2, 4, and 10 µM) of either His-DGAP1(161-822) or in the presence of 10 µM BSA or 1µM of the catalytic domain of human p50RhoGAP. The results of the in vitro assays are plotted as the concentrations of GTP remaining after the times indicated for A and B or after 45 minutes for C. GTP concentrations were determined by reverse phase HPLC.

cortex, crowns, filopods, and accumulated in the leading fronts of the cells. DGAP1-deficient G10– cells were clearly distinguishable from AX2 cells with regard to the cell shape and F-actin staining. Many DGAP1-mutant cells developed a prominent ectoplasmic zone that was strongly labelled with TRITC-phalloidin. This ectoplasmic area, devoid of organelles, was either organised as an exaggerated leading edge or as a rim around the whole cell periphery (Fig. 4B, middle panel). Other G10– cells developed numerous microspikes or long filopods (Fig. 4B, lower panel). Large and multi-nucleate DGAP1-overexpressing cells of transformant G2++ showed a smooth continuous cortical layer of actin and intracellular actin patches, but in contrast to DGAP1-null cells, the accumulation of F-actin to the leading edge or the formation of membrane ruffles or filopodia was largely suppressed. These results demonstrate that DGAP1-expression affects cell shape and organisation of F-actin. The lack of DGAP1 induced the formation of large leading edges, membrane ruffles, and filopodia, whereas DGAP1 overexpression repressed the formation of these structures.

Lack of DGAP1 leads to an increased F-actin content

The bright TRITC-phalloidin staining of DGAP1-null cells as exemplified for transformant G10– in Fig. 4, also indicated that this mutant had a higher F-actin content than AX2 wild-type cells. This indication was confirmed by a quantitative analysis of fluorescence profiles using confocal microscopy and by averaging of data collected from a population of cells. Fig. 5A, shows line scans normalised with respect to cell diameters. Quantification of the fluorescence intensities of AX2 wild-type cells and DGAP1-null mutant G10– revealed a 1.75-fold increase in the total fluorescence in G10– cells. Taking into account that AX2 wild-type and DGAP1-null cells express the same amount of total actin as determined in western blots labelled with anti-actin antibodies (Fig. 5B), our results show that the lack of DGAP1 protein resulted in elevated levels of F-actin. To verify this observation, AX2 wild-type, G10– DGAP1-null, and G2++ DGAP1-overexpressing cells were lysed, and the amount of actin in 100,000 ***g*** pellets and supernatants was quantified in immunoblots labelled with anti-actin antibody mAb 224-236-1. Relative to AX2 wild-type, G10– DGAP1-null cells harbored 40% more actin on the average (F-actin) in the pellet, and the actin fraction in the supernatant (G-actin and short F-actin filaments) was reduced accordingly (Fig. 5C). In DGAP1-overexpressing cells the F-actin content in the pellet was found to be 17% on the average lower when compared to the F-actin content in the pellet of AX2 wild-type cells. Taken together, these results demonstrate that DGAP1 plays an important role in regulating the G-actin/F-actin equilibrium in *Dictyostelium*.

Monitoring the dynamics of actin structures in living DGAP1-null cells using GFP-actin fusions

The microfilament system in the cell cortex of highly motile cells such as *D. discoideum* is subject to rapid re-organisation, either spontaneously or in response to external signals (Gerisch et al., 1993). In order to monitor the influence of DGAP1-deficiency on the actin dynamics in living cells, actin that was tagged at its N terminus with green fluorescent protein (GFP) was expressed in DGAP1-null G10– cells under control of the actin 15 promoter. After selection with G418, several independent transformants expressing GFP-actin were isolated. The amount of GFP-actin relative to total actin in transformant G10-GFPA, which was used for all experiments, was found to be similar to the average amount of GFP-actin

expressed in the AX2-derived strain AX2-GFPA, expressing the same GFP-actin construct (Westphal et al., 1997). Thus, growth-phase cells of strains AX2-GFPA and G10-GFPA moving on a glass surface were comparable employing a double view microscope for simultaneous recording of phase-contrast and fluorescent images. In freely moving AX2-GFPA control cells, GFP-actin was distributed in filopodia, lamellipodia, and in crown-shaped extensions at the dorsal side of the cell surface (Fig. 6A). Active protrusion of a leading edge was invariably associated with a locally elevated GFP-fluorescence. This correspondence was also seen in G10-GFPA cells. However, these cells were clearly distinguishable from AX2-GFPA control cells by the brighter fluorescence in their cortical regions. These results are in agreement with those obtained after labeling of DGAP1-null cells with TRITC-phalloidin as shown in Figs 4, 5A.

Cells of strain G10-GFPA such as the one depicted in Fig. 6B, showed intense membrane ruffling. These ruffles were completely re-organised within a few seconds. Other G10-GFPA cells such as the one shown in Fig. 6C, moved with a large leading edge over the substratum, rounded up after 50 seconds in the recorded sequence, and eventually extended numerous filopods at 85 seconds (Fig. 6C). Frequently G10-GFPA cells were observed that first formed ruffles or migrated with an extended leading edge and then started to extend filopodia. These results suggest that the rapid re-organization of the F-actin cytoskeleton in DGAP1-null cells is not organised in a hierarchical manner in which filopod formation precedes lamellipodia formation as it has been shown for mammalian cells (Chant and Stowers, 1995; Nobes and Hall 1995), but is rather subject to continuous re-modeling.

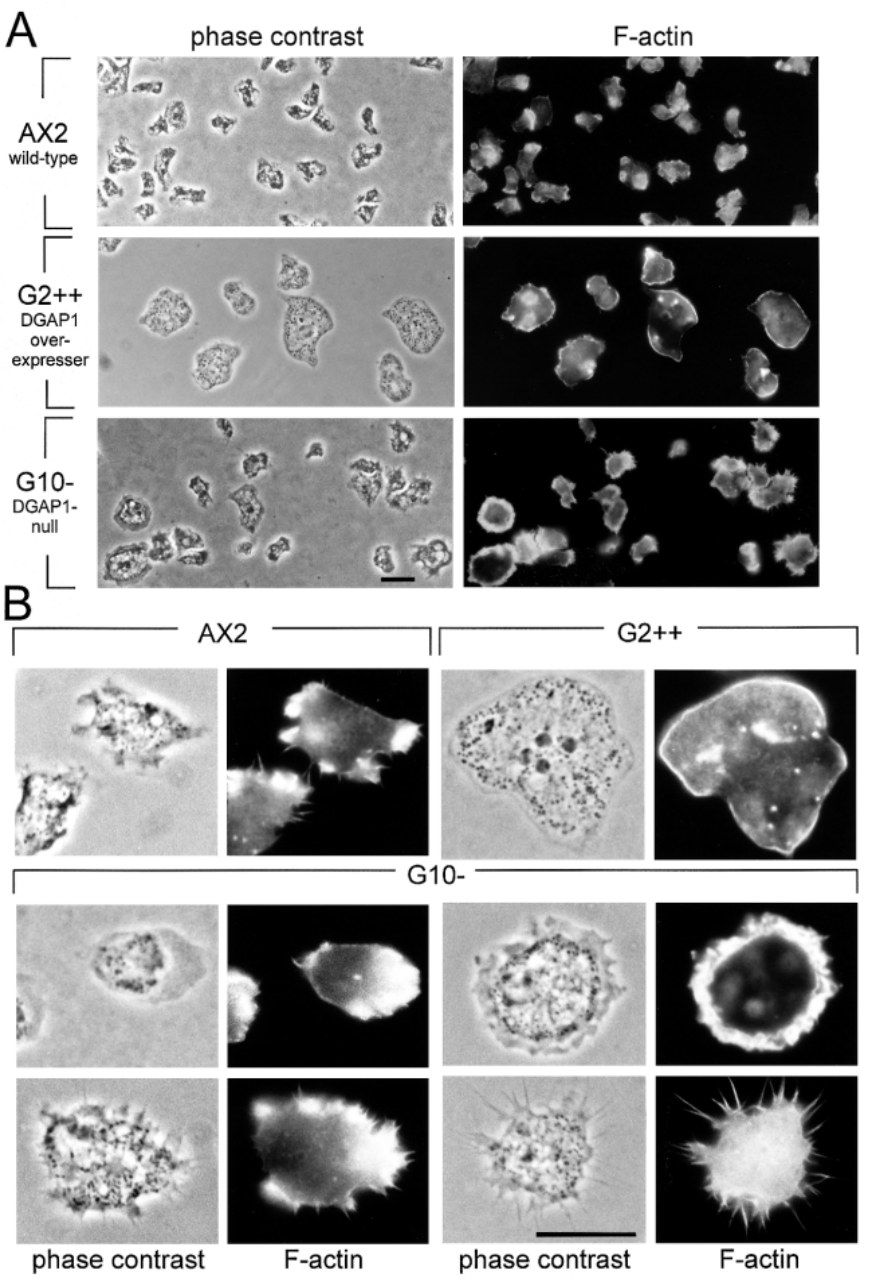

Fig. 4. Cell morphology and organisation of F-actin in wild-type cells and DGAP1-mutants. (A,B) Phase contrast (left rows) and fluorescence (right rows) images of fixed cells from the AX2 wild-type, of DGAP1-null mutant G10–, and of DGAP1-overexpresser G2++ that were labelled with TRITC-phalloidin to visualise F-actin. (A) Low magnification overview. (B) High magnification of individual cells. Bars, 10 μm.

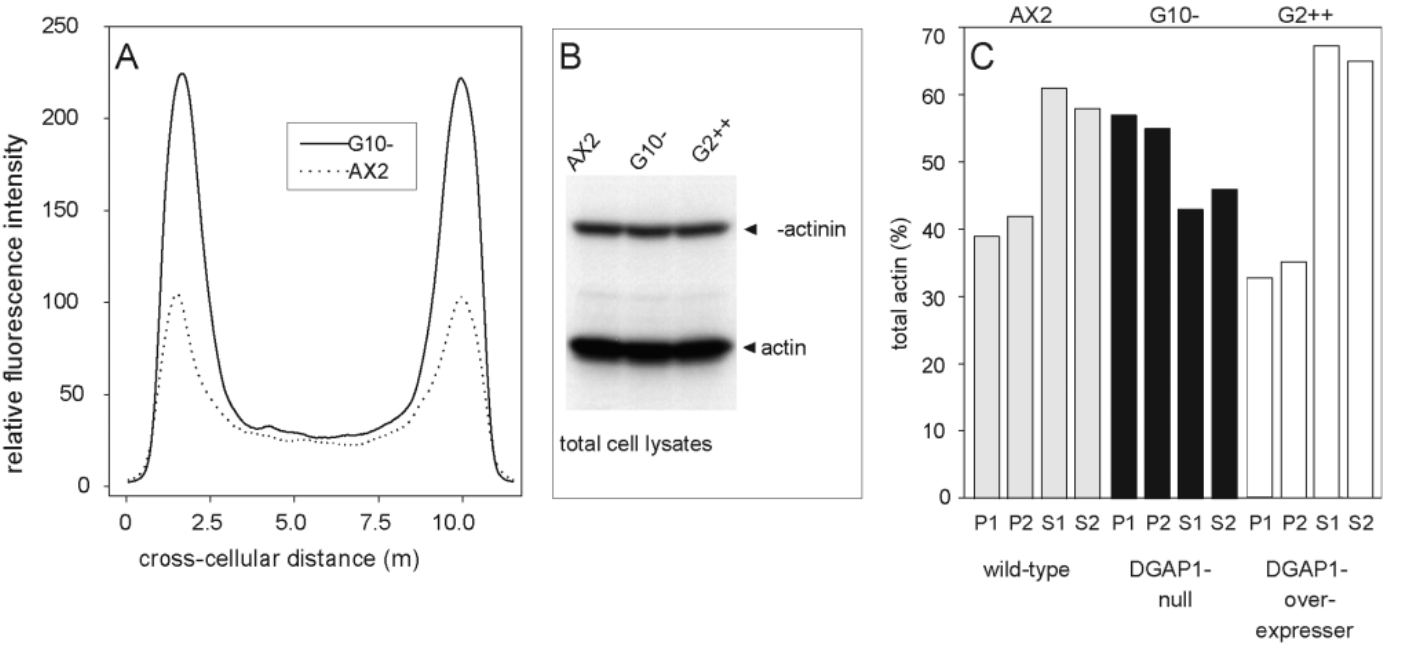

Fig. 5. Altered F-actin content in DGAP1-null mutants. (A) Quantification of F-actin in AX2 wild-type cells and in DGAP1-null mutant G10– employing confocal microscopy. Growth-phase cells of both strains were allowed to adhere to coverslips, the cells fixed, and labelled for F-actin with TRITC-conjugated phalloidin. Confocal sections of 50 randomly chosen cells were recorded for each cell line in a distance of 5 μm above the glass surface and normalised in respect to their cell diameters. The normalised intensity profiles for each cell line are shown. DGAP1-overexpressing G2++ cells were excluded from these analyses because of their multi-nucleate phenotype. (B) Total cellular proteins of the AX2 wild-type, DGAP1-null mutant G10–, and DGAP1-overexpresser G2++ corresponding to 2×10^5 wild-type cells were loaded per lane, subjected to SDS-PAGE, blotted onto nitrocellulose, and labelled with iodinated anti-actin mAb 221-236-1 and anti-α-actinin mAb 47-18-9 antibodies. Quantification of ^{125}I-labelled bands with a phospho imager showed that AX2 wild-type, G10– DGAP1-null, and G2++ DGAP1 overexpressing cells expressed the same amount of total actin. The actin-specific signals were normalised to the α-actinin signals to account for differences in sample loading between lanes. (C) Quantification of actin in AX2 wild-type, G10– DGAP1-null and G2++ DGAP1 overexpressing cells in sedimentation assays. The cells were lysed, and 200 μl samples corresponding to 4×10^5 cells subjected to high speed centrifugation. The actin content is expressed as the percentage of total actin in pellet (P1, P2) or supernatant (S1, S2) fractions, and was determined by quantification of actin-labelled bands in immunoblots. The bars shown represent values of two independent experiments.

DGAP1 expression inversely correlates with cell motility

We have shown previously, that DGAP1-null cells form significantly faster growing colonies on bacterial lawns (Faix and Dittrich, 1996). This phenotype was rescued to the wild-type behaviour by the ectopic expression of the complete *Dgap1* cDNA. These data indicated that DGAP1 is involved in growth control of *D. discoideum* by regulating phagocytosis, a process that is accompanied by re-organisation of the microfilament system (Maniak et al., 1995). To directly test whether DGAP1 regulates phagocytosis in *D. discoideum*, the uptake of fluorescently labelled yeast particles by DGAP1-null, wild-type, and DGAP1-overexpressing cell lines was compared. The rate of uptake in DGAP1-null mutant G10– was slightly lower than in AX2 wild-type cells (Fig. 7A), and the uptake rate in transformant G2++ that overexpresses DGAP1 protein 3-fold, was reduced to approximately 75% of the wild-type rate. We also determined the generation times of AX2, G10– and G2++ cells growing on bacterial lawns using time-lapse video microscopy, since faster growth on bacteria should be accompanied by a shorter generation time. The generation times were 202±58 minutes for AX2, 219±60 minutes for the DGAP1-null mutant G10–, and 321±61 minutes for the DGAP1-overexpressing cell line G2++ (Fig. 7B). These data are in line with the measured yeast uptake rates of the DGAP1-mutants and collectively provide evidence against a direct correlation between DGAP1 expression and phagocytosis or the growth rate. The finding that DGAP1-overexpressing G2++ cells showed defects in two actin-based processes, the phagocytosis of bacteria and the growth rate, is consistent with the observation that re-organisation of the actin cytoskeleton is impaired in this mutant (Fig. 4B, upper right panel).

The analysis of time lapse recordings also revealed, however, that DGAP1 expression affects cell motility, since DGAP1-null cells migrated faster in bacterial lawns than AX2 wild-type cells. The motility of these three cell lines migrating on a glass surface were determined in nutrient medium using a quantitave motility assay. The determined rates of cell motility were 2.5±1.3 μm/minute for AX2 wild-type cells, 4.7±1.7 μm/minute for cells of DGAP1-null transformant G10–, and 1.5±0.9 μm/minute for cells of DGAP1-overexpressing transformant G2++ (Fig. 8). These results demonstrate a inverse correlation between DGAP1 expression and cell motility, and indicate that DGAP1 is involved in the signalling pathway controlling cell migration.

DISCUSSION

In the present study, we showed that *D. discoideum* DGAP1, a protein related in sequence to RasGTPase-activating proteins,

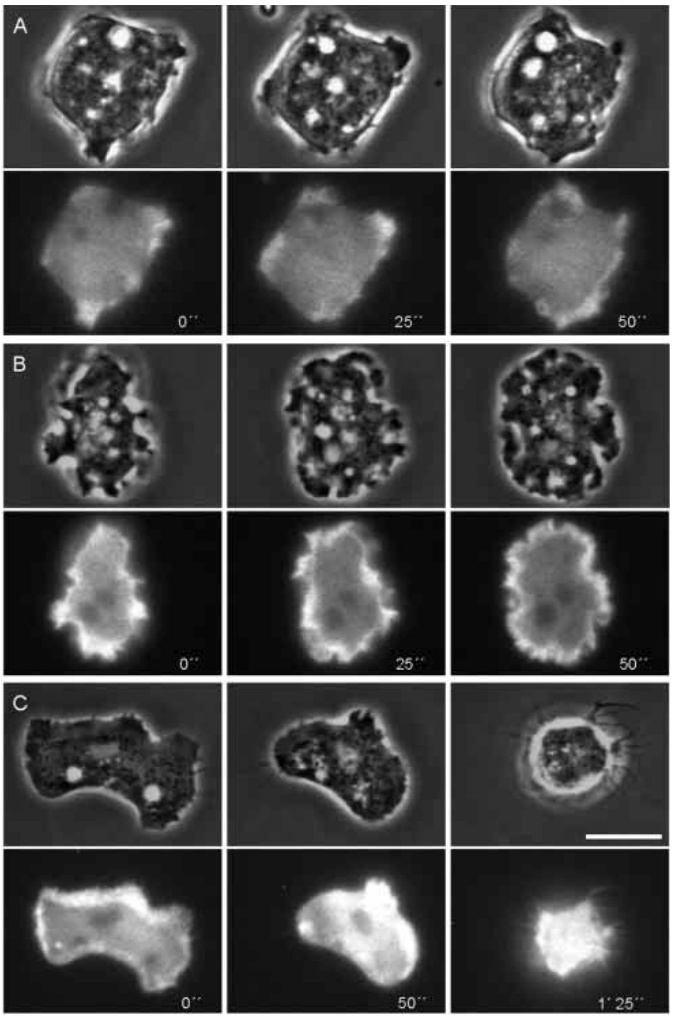

Fig. 6. Comparison of GFP-actin dynamics and cell morphology in living cells from control strain AX2-GFPA (A) and of DGAP1-deficient mutant G10-GFPA (B and C). GFP-actin redistributed to protrusions of the surfaces of the cells from both cell lines, but was more prominent in HG1690 cells. (B) Many cells of strain G10-GFPA showed brightly fluorescent membrane ruffles that were rapidly re-organised. The time course shown in C, illustrates another G10-GFPA cell that first actively protruded a leading edge (left panel), than rounded up (middle panel), and eventually formed many filopods (right panel). The cells shown have been harvested during the exponential growth phase and were allowed to migrate over a glass surface coated with BSA. Phase contrast (upper rows) and fluorescence images (lower rows) were recorded simultaneously with a double view microscope. The exposure time for each fluorescence image was 1 second. The numbers indicates time in seconds of the recorded sequences. Bar, 5 μm. Time lapse movies of the shown cells can be downloaded from the World Wide Web (www.biochem.mpg.de/~faix/home.htm).

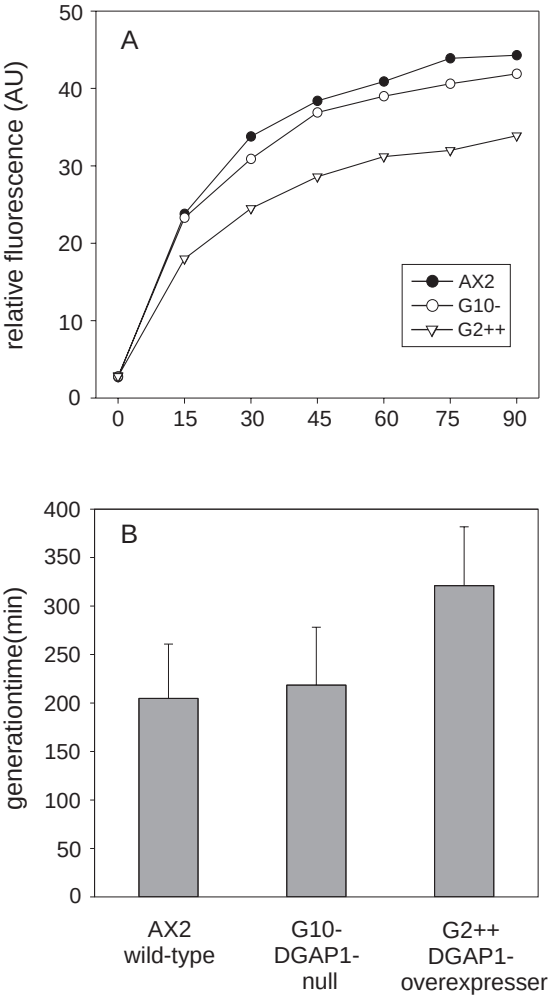

Fig. 7. Phagocytosis rates and generation times of wild-type cells and DGAP1-mutants. (A) The rates of phagocytosis in the wild-type AX2, in DGAP1-null transformant G10–, and in the DGAP1-overexpressing cell line G2++ that overexpresses DGAP1 protein three-fold are compared. Data represent mean values of three independent experiments done in parallel with wild-type and mutant cell lines. Since multi-nucleate DGAP1-overexpressing transformant G2++ had an increased cell volume, the data shown were normalised to protein content. (B) Generation times of the same strains on bacteria. Mean values shown have been calculated from 150 cell division determined for each cell line. Error bars indicate standard deviations. Generation times for G2++ cells were significantly different from both AX2 and G10– cells ($P<10^{-4}$, two-sided *t*-test). The difference between AX2 and G10– strains was marginally significant ($0.1>P>0.05$).

failed to promote GTP-hydrolysis of both, human H-Ras and of *D. discoideum* RasG, thereby demonstrating that DGAP1 lacks in vitro RasGAP activity. These results are not consistent with those of Lee et al. (1997) who reported that *D. discoideum* DdRasGAP1, which is identical with DGAP1, stimulated GTP-hydrolysis of *D. discoideum* RasD protein. However, as shown in Fig. 9, DGAP1 carries amino-acid substitutions in two regions of the RasGAP-related domain, which are invariant in all other RasGAPs like *Schizosaccharomyces pombe* Sar1. These conserved residues are considered to be essential for the catalytic activity of RasGAPs (Weissbach et al., 1994; Ahmadian et al., 1996; Scheffzek et al., 1996; 1997a). In the first region an arginine residue referred to as the arginine finger, which corresponds to Arg^{789} in p120RasGAP (Scheffzek et al., 1996) is replaced in DGAP1 by a lysine residue (Lys^{259}). The second region, denoted as the FLR-motif (^{901}Phe-Leu-Arg^{903} in p120RasGAP), is replaced by ^{404}Tyr-Tyr-Arg^{406} in DGAP1 (Fig. 9). The three-dimensional structure of the complex between the human H-Ras*GDP and the catalytic domain of

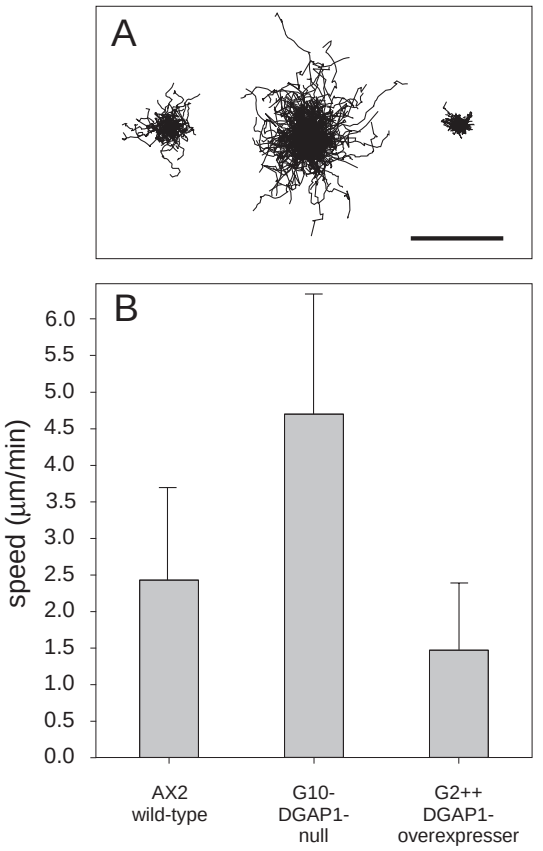

Fig. 8. Inverse correlation of DGAP1-expression and cell motility. (A) Individual tracks of migrating AX2 wild-type cells (left), DGAP1-null transformant G10– (middle), and DGAP1-overexpressing transformant G2++ (right) in growth medium. The tracks were recorded for 30 minutes, superimposed, and plotted to a common origin using an image processing system. Bar represents 200 µm. (B) Quantification of cell motility for the same cell strains in growth medium. The bars show the mean values for the cell velocities from 15 experiments for each cell line. The error bars indicate the standard deviation of the mean. The differences between these strains were highly significant ($P<10^{-4}$, two-sided *t*-test).

human p120RasGAP (GAP-334) has been solved at a resolution of 2.5 Å in the presence of aluminum fluoride that mimics the γ-phosphate group of GTP (Scheffzek et al., 1997b). The structure shows that the side chain of the finger arginine (Arg^{789}) of GAP-334 is oriented into the active site of Ras to neutralise developing charges in the transition state of GTP-hydrolysis. Arg^{903} in p120RasGAP of the FLR-motif is not directly involved in catalysis, but is presumably responsible for the correct positioning of the catalytic arginine. A systematic mutational analysis in p120RasGAP and neurofibromin I (NF-1), another human RasGAP, by Ahmadian et al. (1997b) revealed that conversion of the catalytic finger arginine to other amino-acid residues, even to a conserved lysine residue, resulted in the loss of catalytic activity by NF-1 and p120RasGAP, confirming that the finger arginine is essential for catalytic activity of RasGAPs. Thus, DGAP1 that has amino-acid substitutions in the FLR motif, and in particular lacks the catalytic arginine residue, is therefore not expected to have a RasGAP activity.

In this regard, DGAP1 is similar to the mammalian IQGAPs which are also devoid of RasGAP activity (Weissbach et al., 1994; Brill et al., 1996; Hart et al., 1996). These proteins lack the catalytic finger arginine and show amino-acid substitutions in the FLR-motif of the GAP-related domain (Fig. 9). In addition, we have shown that DGAP1, like the mammalian IQGAPs, interacts with activated forms of Rho family GTPases, in particular with human Rac1 and its closely related homologue Rac1A of *D. discoideum*. DGAP1 binds directly to Rac1A and almost the entire DGAP1 protein (residues 161-822) is required for strong binding to activated Rac1A. We demonstrate that DGAP1, similar to IQGAP1 and IQGAP2, lacks in vitro RacGAP activity (Fig. 3). Taking together, these results suggest that DGAP1 of *D. discoideum* is structurally and functionally related to the mammalian IQGAPs. Nevertheless, the biochemical properties of DGAP1 and the IQGAPs are not completely identical. Unlike IQGAP1 (Bashour et al., 1997), full-length recombinant His-DGAP1(1-822) does not co-sediment with F-actin. This finding is not surprising, since the binding of F-actin to IQGAP1 is mediated by a calponin-homology domain in the N-terminal part of this protein. The N-terminal halve containing this domain is missing in DGAP1. Further, IQGAP2 was shown to inhibit both the intrinsic and RhoGAP mediated GTP hydrolysis of Cdc42 and Rac1, indicating that IQGAP keeps Cdc42 and Rac1 in their active, GTP-bound forms (Brill et al., 1996), whereas DGAP1 showed no influence on the intrinsic GTPase activities of human Rac1 and *D. discoideum* Rac1A. Another difference is the lack of DGAP1 interaction with the activated form of Cdc42, that has been reported to be the strongest ligand of mammalian IQGAPs (Hart et al., 1996; Brill et al., 1996; McCallum et al., 1996; Kuroda et al., 1996). However, this lack of binding might not be surprising, since to date considerable efforts by our and other laboratories to identify a homologue of human or yeast Cdc42 in *D. discoideum* using multiple genetic and immunological approaches have not been successful. This may indicate that either the Cdc42 protein in *D. discoideum* has not been detected because it is quite divergent from its mammalian and yeast counterparts, or that one of the multiple Rac proteins possesses a Cdc42-like function in *D. discoideum*. Eight *rac* genes have been described so far for *D. discoideum* (Bush et al., 1993; Larochelle et al., 1996). The *rac* genes (*rac1A*, *rac1B*, *rac1C*) encode proteins with more that 90% identity to each other and more that 85% identity to human Rac1, whereas the other members (*racA*, *racB*, *racC*, *racD*, and *racE*) encode proteins with 46-74% identity to human Rac1 (Bush et al., 1993; Larochelle et al., 1996).

An important result of this study was the finding of different strength of DGAP1-binding to the three Racs of *D. discoideum* we have tested for interaction with DGAP1. The strongest interaction was found with activated Rac1A, and an intermediate strength with RacE that showed no dependence on the guanine nucleotide bound to RacE. Lastly, almost no binding of DGAP1 was seen to RacC (Fig. 2B), indicating that DGAP1 interacts specifically only with a subset of the Rac proteins present in *D. discoideum*. The interpretation of the data presented here raise a number of interesting of questions. Which of the eight different Rac-proteins interact specifically in their activated forms with DGAP1? As Rac1A is most closely related to Rac1B and Rac1C, it is likely that DGAP1

also interacts with these highly related Rac proteins. No clear-cut conclusion can be drawn from the binding experiments obtained with RacE to DGAP1, since the DGAP1-RacE interactions, although significant, were independent of the guanine nucleotide bound to RacE. RacE has been shown to be specifically involved in cytokinesis (Larochelle et al., 1996). The ectopic expression of either wild-type RacE or a constitutively active V20RacE mutant effectively rescued the cytokinesis defect of RacE-null cells, whereas expression of a dominant-negative N25RacE mutant protein did not (Larochelle et al., 1997). These results lead to the conclusion that cytokinesis in *D. discoideum* only requires the activation of RacE by GTP, and not the inactivation of RacE by hydrolysis of GTP. A 3-fold DGAP1 overexpression leads to a similar defect in cytokinesis (Faix and Dittrich, 1996). Thus, it is reasonable to assume that DGAP1 overexpression may sequester RacE from the signalling pathway involved in cytokinesis and therefore mimic a cell line depleted for RacE. The observation that RacC bound poorly to DGAP1 suggests that RacC is involved in a pathway distinct from that of Rac1A and of RacE, and is in agreement with the finding that ectopic expression of RacC is not sufficient to rescue the cytokinesis defect of RacE-null cells (Larochelle et al., 1997). Taken together, these results raise another question. What other protein(s) interact specifically with RacC or the other Racs that do not interact with DGAP1? A possible candidate protein is the recently reported GAPA from *D. discoideum* (Adachi et al., 1997). GAPA shows 50% overall identity with DGAP1 and carries amino-acid substitutions in the GAP-related domain, in particular the catalytic finger arginine, necessary for RasGAP activity (Fig. 9). Thus, it is likely that GAPA acts as another IQGAP-related Rac effector in *D. discoideum*.

In this study we have established a functional connection between DGAP1, activated Rac1A, the actin cytoskeleton, and cell motility in *D. discoideum*. DGAP1-null mutants are remarkable because they display striking differences in cell shape and cytoskeletal architecture when compared to wild-type cells. The formation of cellular projections is largely suppressed in DGAP1-overexpressing cells, whereas DGAP1-null cells either develop unusually numerous filopods, membrane ruffles, or a prominent ectoplasmic zone. This exaggerated area, devoid of organelles, is either organised as a rim around the whole cell periphery or extends far beyond the leading edge (Fig. 4, middle panel). This phenotype of DGAP1-null mutants is quite distinct from DGAP1 overexpressing cells or from AX2 wild-type cells, in which this organelle-free region is restricted to the leading cell margin (Gerisch et al., 1995). The hyaline zone of DGAP1-null cells is full of actin filaments as demonstrated with TRITC-phalloidin labelling of these cells. In support of these results, we show that elimination of DGAP1 causes an increase in the level of F-actin (Fig. 4, middle panel). Taken together, these findings indicate that DGAP1 is involved in the control of the actin polymerisation-de-polymerisation cycle. Since it binds to activated members of the Rho family of GTPases, which have been shown to be implicated in the re-modelling of the cytoskeleton in mammalian cells (Ridley et al., 1992; Nobes and Hall, 1995), and its absence leads to an increased polymerisation of cortical actin in vivo, it seems reasonable to assume that DGAP1 is integrated in a signal transduction pathway that is involved in the de-polymerisation of filamentous actin.

Motile eukaryotic cells contain an impressive variety of proteins that modulate the organisation and function of the microfilament system (Pollard and Cooper, 1986; Luna and Condeelis, 1990; Cooper, 1991; Stossel, 1993). The faster migration observed in DGAP1-deficient cells could be mediated through capping proteins that bind to the barbed ends of actin filaments and prevent the addition of actin monomers, and by severing proteins that fragment and cap actin filaments (Hartwig and Kwiatkowski, 1991). In support of this idea is the overexpression of Cap32/34 in *Dictyostelium* cells (Hug et

```
Hs IQGAP1   LIFQMPQNKSTKFMDSVIFTLYNYASNQREEYLLLRLFKTALQEEIKSKV  1038
Hs IQGAP2   LIFQMPQNKSTKFMDTVIFTLYNYASNQREEYLLLKLFKTALEEEIKSKV   953
Dd DGAP1    LVYLIQPEQMESFLGTVILTLFGDAFTPREEFLLLSLYRLSIQKEMAN-I   251
Dd GAPA     LVTLIQADQMEDFLDTVFLTLFGDDFSPREEFLILSLFRLAIGQEMSR-I   286
Sp Sar1     LVRRVKLFNMDALLQIVMFNIYGNQYESREEHLLLSLFQMVLTTEFEA-T   188

Hs IQGAP1   DQIQEIVIGNPTVIKMVVSFNRGARGQNALRQILAPVVKE-IMDDKSLNI  1087
Hs IQGAP2   DQVQDIVIGNPTVIKMVVSFNRGARGQNTLRQLLAPVVKE-IIDDKSLII  1002
Dd DGAP1    ATVGDFLKADTVLPKMIITYNKRKQGTDYLKAVIGPILSN-V-IKQELNL   299
Dd GAPA     KSAGDLLAVESVVPKMIITYTRRKQGHEFLKQIIAPILENNVVNAPDLNL   336
Sp Sar1     SDVLSLLRANTPVSRMLTTYTRRGPGQAYLRSILYQCIND-VAIHPDLQL   237

Hs IQGAP1   KTDPVDIYKSWVNQMESQTGEASKLPYDVTPEQALAHEEVKTRLDSSIRN  1137
Hs IQGAP2   NTNPVEVYKAWVNQLETQTGEASKLPYDVTTEQALTYPEVKNKLEASIEN  1052
Dd DGAP1    ELKPNLVYAAIISEQEIRTGEKSTLDRNVSHEKALEVPEVTKTIKARVDQ   349
Dd GAPA     ELNAVQVYQNMISEQEIQTGAKSTLNRGLAEDQIIQLKEVQSILEPRVEK   386
Sp Sar1     DIHPLSVYRYLVNTGQLSPSEDDNL---LTNEEVSEFPAVKNAIQERSAQ   284

Hs IQGAP1   MRAVTDKFLSAIVSSVDKIPYGMRFIAKVLKDSLHEKFPDAGEDELLKII  1187
Hs IQGAP2   LRRVTDKVLNSIISSLDLLPYGLRYIAKVLKNSIHEKFPDATEDELLKIV  1102
Dd DGAP1    LISICEQFLDGIISSLNRLPYGIRWICKQIYQIAEKNFTKSTQDETLKVI   399
Dd GAPA     CIQICERFFTGIIQSLNRLPYGIRWICKQIQSIAQKNF-DSKPDEIAKVI   435
Sp Sar1     LLLLTKRFLDAVLNSIDEIPYGIRWVCKLIRNLTNRLFPSISDSTICSLI   334

Hs IQGAP1   GNLLYYRYMNPAIVAPDAFDIIDLSAGGQLTTDQRRNLGSIAKMLQ      1233
Hs IQGAP2   GNLLYYRYMNPAIVAPDGFDIIDMTAGGQINSDQRRNLGSVAKVLQ      1148
Dd DGAP1    GYFIYYRFIQVAMVSPEEYDLVG----REIHPTARKNLINVSKVLQ       441
Dd GAPA     GYFVYYRFINLAIVTPDAFEILD----KELSITSRKNLVNIAKVLQ       477
Sp Sar1     GGFFFLRFVNPAIISPQTSMLLD----SCPSDNVRKTLATIAKIIQ       376
```

Fig. 9. Multiple sequence alignment of the GAP-related domains from IQGAP1, IQGAP2, DGAP1, GAPA, and Sar1/Gap1. Dashes indicate gaps introduced for optimal alignment. The two sites highlighted as white letters against black show amino-acid substitutions of IQGAP1, IQGAP2, DGAPA, and DGAP1 in positions that are considered to be crucial for RasGAP activity and that are invariant in all other RasGAPs, such as Sar1/Gap1. *Hs*, *Homo sapiens*; *Dd*, *Dictyostelium discoideum*, *Sp*, *Schizosaccharomyces pombe*. GenBank accession numbers: IQGAP1, L33075; IQGAP2, U51903; DGAP1, L75794; GAPA, D88027; Sar1/Gap1, S37449.

al., 1995) and of gelsolin in NIH 3T3 fibroblasts (Cunningham et al., 1991) to enhanced motility. A model that provides a functional connection between Rac, capping proteins, and actin re-organisation in human platelets has been proposed by Hartwig et al. (1995). According to this model, Rac activates phosphatidylinositol 4-phosphate 5-kinase that results in transiently elevated levels of phosphatidylinositol 4,5-bisphosphate (PIP_2) which in turn leads to the inactivation of capping proteins, such as gelsolin. The uncapped barbed ends of F-actin filaments are available for the addition of G-actin subunits, which results in the de novo polymerisation of actin (Hartwig et al., 1995). Thus, PIP_2 was considered as a strong candidate for a second messenger regulating actin polymerisation (Schafer et al., 1996). However, no correlation between PIP_2 synthesis mediated by activated Rac1 and actin polymerisation was observed in polymorphonuclear leukocytes or *Dictyostelium* cells (Zigmond et al., 1997). Thus, further investigation will be necessary to determine how DGAP1 is involved in the re-modelling of the microfilament system.

In summary, this report provides a functional link between the small GTPase Rac1A and its effector DGAP1. It demonstrates the important role of DGAP1 in the signal transduction pathways leading to dynamic re-arrangements of the actin cytoskeleton, control of actin filament turnover, and in cell motility. Unravelling the mechanism of how DGAP1 controls the organisation and dynamics of the actin cytoskeleton will be essential to better understand the molecular basis of cell motility.

We thank Dr M. Maniak for advise in performing phagocytosis assays, L. Lindemann for assistance in protein purification, J.-M. Schwartz for image processing, and M. Westphal for transformant HG1662. We are grateful to Drs A. De Lozanne for GST-RacE construct, R. Cool for GST-Rac1 construct, R. Mittal for catalytic domain of p50RhoGAP protein, G. Gerisch and A. Wittinghofer for helpful suggestions, and I. Weber and G. Marriott for reading of the manuscript. This work was supported by the Deutsche Forschungsgemeinschaft.

REFERENCES

Adachi, H., Takahashi, Y., Hasebe, T., Shirouzu, M., Yokoyama, S. and Sutoh, K. (1997). *Dictyostelium* IQGAP-related protein specifically involved in the completion of cytokinesis. *J. Cell Biol*. **137**, 891-898.

Ahmadian, M. R., Wiesmüller, L., Lautwein, A., Bischoff, F. R. and Wittinghofer, A. (1996). Structural differences in the minimal catalytic domains of the GTPase-activating proteins $p120^{GAP}$ and neurofibromin. *J. Biol. Chem.* **271**, 16409-16415.

Ahmadian, M. R., Mittal, R., Hall, A. and Wittinghofer, A. (1997a). Aluminum fluoride associates with the small guanine nucleotide binding proteins. *FEBS Lett*. **408**, 315-318.

Ahmadian, M. R., Stege, P., Scheffzek, K. and Wittinghofer, A. (1997b). Confirmation of the argininie-finger hypothesis for the GAP-stimulated GTP-hydrolysis reaction of Ras. *Nature Struct. Biol*. **4**, 686-689.

Amano, M., Mukai, H., Ono, Y., Chihara, K., Matsui, T., Hamajima, Y., Okawa, K., Iwamatsu, A. and Kaibuchi, K. (1996). Identification of a putative target for Rho as serine-threonine kinase protein kinase N. *Science* **271**, 648-650.

Bashour, A.-M., Fullerton, A. T., Hart, M. J. and Bloom, G. S. (1997). IQGAP1, a Rac and Cdc42-binding protein, directly binds and cross-links microfilaments. *J. Cell Biol*. **137**, 1555-1566.

Boguski, M. S. and McCormick, F. (1993). Proteins regulating ras and its relatives. *Nature* **366**, 643-654.

Braga, V. M. M., Machesky, L. M., Hall, A. and Hotchin, N. A. (1997). The small GTPases Rho and Rac are required for the establishment of cadherin-dependent cell-cell contacts. *J. Cell Biol*. **137**, 1421-1431.

Brill, S., Li, S., Lyman, C. W., Church, D. M., Wasmuth, J. J., Weissbach, L., Bernards, A. and Snijders, A. J. (1996). The Ras GTPase-activating-protein-related human protein IQGAP2 harbors a potential actin binding domain and interacts with calmodulin and Rho family GTPases. *Mol. Cell. Biol*. **16**, 4869-4878.

Burbelo, P. D., Drechsel, D. and Hall, A. (1995). A conserved binding motif defines numerous candidate target proteins for both Cdc42 and Rac GTPases. *J. Biol. Chem.* **270**, 29071-29074.

Bush, J., Franek, K. and Cardelli, J. (1993). Cloning and characterization of seven novel *Dictyostelium discoideum rac*-related genes belonging to the rho family of GTPases. *Gene* **136**, 61-68.

Chant, J. and Stowers, L. (1995). GTPase cascades – Choreographic cellular behavior: movement, morphogenesis, and more. *Cell* **81**, 1-4.

Claviez, M., Pagh, K., Maruta, H., Baltes, W., Fisher, P. and Gerisch, G. (1982). Electron microscopic mapping of monoclonal antibodies on the tail region of *Dictyostelium* myosin. *EMBO J*. **1**, 1017-1022.

Cooper, J. A. (1991). The role of actin polymerization in cell motility. *Annu. Rev. Physiol.* **53**, 585-606.

Cunningham, C. C., Stossel, T. P. and Kwiatkowski, D. J. (1991). Enhanced motility in NHI 3T3 fibroblasts that overexpress gelsolin. *Science* **251**, 1233-1236.

Diekmann, D., Abo, A., Johnston, C., Segall, W. A. and Hall, A. (1994). Interaction of Rac with p67phox and regulation of phagocytic NADPH oxidase activity. *Science* **265**, 531-533.

Djinovic Carugo, K., Bañuelos, S. and Saraste, M. (1997). Crystal structure of a calponin homology domain. *Nature* **4**, 175-179.

Faix, J. and Dittrich, W. (1996). DGAP1, a homologue of rasGTPase activating proteins that controls growth, cytokinesis, and development in *Dictyostelium discoideum. FEBS Lett*. **394**, 251-257.

Faix, J., Steinmetz, M., Boves, H., Kammerer, R. A., Lottspeich, F., Mintert, U., Murphy, J., Stock, A., Aebi, U. and Gerisch, G. (1996). Cortexillins, major determinants of cell shape and size, are actin-bundling proteins with a parallel coiled-coil tail. *Cell* **86**, 631-642.

Fisher, P. R., Merkl, R. and Gerisch, G. (1989). Quantitative analysis of cell motility and chemotaxis in *Dictyostelium discoideum* by using an image processing system and a novel chemotaxis chamber providing stationary chemical gradients. *J. Cell Biol*. **104**, 973-984.

Gerisch, G. (1960). Zellfunktionen und Zellfunktionswechsel in der Entwicklung von *Dictyostelium discoideum*. I. Zellagglutination und Induktion der Fruchtkörperpolarität. *Roux's Arch. Entwicklungsmech.* **152**, 632-654.

Gerisch, G., Albrecht, R., deHostos, E., Wallraff, E., Heizer, C., Kreitmeier, M., and Müller-Taubenberger, A. (1993). Actin-associated proteins in motility and chemotaxis of *Dictyostelium* cells. In *Cell Behaviour: Adhesion and Motility* (ed. G. Jones, C. Wigley and R. Warn), pp. 297-315. The Society of Experimental Biology, Cambridge, UK.

Gerisch, G., Albrecht, R., Heizer, C., Hodgkinson, S. and Maniak, M. (1995). Chemoattractant-controlled accumulation of coronin at the leading edge of *Dictyostelium* cells monotored using a green fluorescent protein-coronin fusion. *Curr. Cell Biol*. **5**, 1280-1285

Hart, M. J., Callow, M. G., Souza, B. and Polakis, P. (1996). IQGAP1, a calmodulin-binding protein with a rasGAP-related domain, is a potential effector for Cdc42Hs. *EMBO J.* **15**, 2997-3005.

Hartwig, J. H. and Kwiatkowski, D. J. (1991). Actin-binding proteins. *Curr. Opin. Cell Biol.* **3**, 87-97.

Hartwig, J. H., Bokoch, G. M., Carpenter, C. L., Janmey, P. A., Taylor, L. A., Toker, A. and Stossel, T. P. (1995). Thrombin receptor ligation and activated rac uncap actin filament barbed ends through phosphoinositide synthesis in permeabilized human platelets. *Cell* **82**, 643-653.

Hug, C., Jay, P., Reddy, I., McNally, J., Bridgman, P., Eison, E. and Cooper, J. (1995). Capping protein level influence actin assembly and cell motility in *Dictyostelium. Cell* **81**, 591-600.

Humbel, B. M. and Biegelman, E. (1992). A preparation protocol for postembedding immunoelectron microscopy of *Dictyostelium discoideum* with monoclonal antibodies. *Scanning Microsc*. **6**, 817-825.

Imai, Y., Miyake, S., Hughes, D. A. and Yamamoto, M. (1991). Identification of a GTPase-activating protein homolog in *Schizosaccharomyces pombe*. *Mol. Cell. Biol*. **11**, 3088-3094.

John, J., Sohmen, R., Feuerstein, J., Linke, R., Wittinghofer, A. and Goody, R. S. (1990). Kinetics of interaction of nucleotides with nucleotide-free H-ras p21. *Biochemistry* **29**, 6058-6065.

Khosla, M., Spiegelman, G. B. and Weeks, G. (1996). Overexpression of an

activated *rasG* gene during growth blocks the initiation of *Dictyostelium* development. *Mol. Cell. Biol*. **16**, 4156-4162.

Kimura,K., Ito, M., Amano, M., Chihara, K., Fukata, M., Nakafuku, M., Yamamori, B., Feng, J., Nakano, T., Okawa, K., Iwamatsu, A. and Kaibuchi, K. (1996). Regulation of myosin phosphatase by Rho and Rho-associated kinase (Rho-kinase). *Science* **273**, 245-248.

Kozma, R., Ahmed, S., Best, A. and Lim, L. (1995). The Ras-related protein Cdc42Hs and bradykinin promote formation of peripheral actin microspikes and filopodia in Swiss 3T3 fibroblasts. *Mol. Cell Biol*. **15**, 1942-1952.

Kuroda, S., Fukata, M., Kobayashi, K., Nakafuku, M., Nomura, N., Iwamatsu, A. and Kaibuchi, K. (1996). Identification of IQGAP as a putative target for the small GTPases, Cdc42 and Rac1. *J. Biol. Chem*. **271**, 23363-23367.

Lancaster, C. A., Taylor-Harris, P. M., Self, A. J., Brill, S., van Erp, H. E. and Hall, A. (1994). Characterization of rhoGAP. A GTPase-activating protein for rho-related small GTPases. *J. Biol. Chem*. **269**, 1137-42.

Larochelle, D. A., Vithalani, K. K. and De Lozanne, A. (1996). A novel member of the rho family of small GTP-binding proteins is specifically required for cytokinesis. *J. Cell Biol.* **133**, 1321-1329.

Larochelle, D. A., Vithalani, K. K. and De Lozanne, A. (1997). Role of *Dictyostelium* racE in cytokinesis: Mutational analysis and localization studies by use of green fluorescent protein. *Mol. Biol. Cell* **8**, 935-944.

Lee, S., Escalante, R. and Firtel, R. A. (1997). A RasGAP is essential for cytokinesis and spatial patterning in *Dictyostelium*. *Development* **124**, 983-996.

Lenzen, C., Cool, R. H., Prinz, H., Kuhlmann, J. and Wittinghofer, A. (1998). Kinetic analysis by fluorescence of the interaction between Ras and the catalytic domain of the guanine nucleotide exchange factor Cdc25(Mm). *Biochemistry* **37**, 7420-7430.

Luna, E. J. and Condeelis, J. S. (1990). Actin-associated proteins in *Dictyostelium discoideum*. *Dev. Gen.* **11**, 328-332.

Maniak, M., Rauchenberger, R., Albrecht, R., Murphy, J. and Gerisch, G. (1995). Coronin involved in phagocytosis: Dynamics of particle-induced relocalization visualized by a green fluorescent protein tag. *Cell* **83**, 915-924.

Manser, E., Leung, T., Salihuddin, H., Tan, L. and Lim, L. (1993). A non-receptor tyrosine kinase that inhibits the GTPase activity of p21Cdc42. *Nature* **363**, 364-367.

Manser, E., Chong, C., Zhao, Z.S., Leung, T., Michael, G., Hall, C. and Lim, L. (1995). Molecular cloning of a new member of the p21-Cdc42/Rac-activated kinase (PAK) family. *J. Biol. Chem*. **270**, 25070-25078.

Martin, G. A., Bollag, G., McCormick, F. and Abo, A. (1995). A novel serine kinase activated by rac1/Cdc42Hs-dependent autophosphorylation is related to Pak65 and STE20. *EMBO J*. **14**, 1970-1978.

Matsui, T., Amano, M., Yamamoto, T., Chihara, K., Nakafuku, M., Ito, M., Nakano, T., Okawa, K., Iwamatsu, A. and Kaibuchi, K. (1996). Rho-associated kinase, a novel serine/threonine kinase, as putative target for small GTP-binding protein Rho. *EMBO J*. **15**, 2208-2216.

McCallum, S. J., Wu, W. J. and Cerione, R. A. (1996). Identification of a putative effector for Cdc42Hs with high sequence similarity to the RasGAP-related protein IQGAP1 and a Cdc42Hs binding partner with similarity to IQGAP2. *J. Biol. Chem*. **271**, 21732-21737.

Nellen, W., Silan, C. and Firtel, R. A. (1984). DNA-mediated transformation of *Dictyostelium discoideum*: Regulated expression of an actin gene fusion. *Mol. Cell. Biol*. **4**, 2890-2898.

Nobes, C. D. and Hall, A. (1995). Rho, rac, and cdc42 GTPases regulate the assembly of multimolecular focal complexes associated with actin stress fibers, lamellipodia, and filopodia. *Cell* **81**, 53-62.

Pollard, T. D. and Cooper, J. A. (1986). Actin and actin-binding proteins. A critical evaluation of mechanisms and functions. *Annu. Rev. Biochem*. **55**, 987-1035.

Ridley, A. and Hall, A. (1992). The small GTP-binding protein rho regulates assembly of focal adhesions and actin stress fibers in response to growth factors. *Cell* **70**, 389-399.

Ridley, A. J., Paterson, H. F., Johnston, C. L., Diekmann, D. and Hall, A. (1992). The small GTP-binding protein ras regulates growth factor-induced membrane ruffling. *Cell* **70**, 401-410.

Robbins, S. M., Williams, J. G., Spiegelman, G. B. and Weeks, G. (1992). Cloning and characterization of the *Dictyostelium discoideum rasG* genomic sequence. *Biochim. Biophys. Act.* **1130**, 85-89.

Schafer, D. A., Jennings, P. B. and Cooper, J. A. (1996). Dynamics of capping protein and actin assembly in vitro: Uncapping of barbed ends by phosphoinositides. *J. Cell Biol.* **135**, 169-179.

Scheffzek, K., Lautwein, A., Kabsch, W., Ahmadian, M. R. and Wittinghofer, A. (1996). Crystal structure of the GTPase-activating domain of human p120GAP and implications for the interaction with Ras. *Nature* **384**, 591-596.

Scheffzek, K., Ahmadian, M. R., Lautwein, A., Scherer, A., Franken, S. and Wittinghofer, A. (1997a). Crystallization and preliminary x-ray crystallographic study of the ras-GTPase-activating domain of human p120gap. *Proteins* **27**, 315-318.

Scheffzek, K., Ahmadian, M. R., Kabsch, W., Wiesmüller, L., Lautwein, A., Schmitz, F. and Wittinghofer, A. (1997b). The Ras-RasGAP complex: Structural basis for GTPase activation and its loss in oncogenic Ras mutants. *Science* **277**, 333-338.

Schleicher, M., Noegel, A., Schwarz, T., Wallraff, E., Brink, M., Faix, J., Gerisch, G. and Isenberg, G. (1988). A *Dictyostelium* mutant with severe defects in α-actinin: its characterisation using cDNA probes and monoclonal antibodies. *J. Cell. Sci*. **90**, 59-71.

Segall, J. E., Fisher, P. R. and Gerisch, G. (1987). Selection of chemotaxis mutants of *Dictyostelium discoideum. J. Cell Biol*. **10**, 151-161.

Stossel, T. P. (1993). On the crawling of animal cells. *Science* **260**, 1086.

Symons, M., Derry, J. M. J., Karlak, B., Jiang, S., Lemahieu, V., McCormick, F., Franke, U. and Abo, A. (1996). Wiskott-Aldrich Syndrome protein, a novel effector for the GTPase Cdc42Hs, is implicated in actin polymerization. *Cell* **84**, 723-734.

Tucker, J., Sczakiel, G., Feuerstein, J., John, J., Goody, R. S. and Wittinghofer, A. (1986). Expression of p21 proteins in *Escherichia coli* and stereochemistry of the nucleotide-binding site. *EMBO J*. **5**, 1351-1358.

Van Aelst, L., Joneson, T. and Bar-Sagi, D. (1996). Identification of a novel Rac1-interacting protein involved in membrane ruffling. *EMBO J*. **15**, 3778-3786.

Van Aelst, L. and D'Souza, C. (1997). Rho GTPases and signaling networks. *Gen. Dev.* **11**, 2295-2322.

Wang, Y., Boguski, M., Riggs, M., Rodgers, L. and Wigler, M. (1991). *Sar1*, a gene from *Schizosaccharomyces pombe* encoding a protein that regulates ras. *Cell Regulation* **2**, 453-465.

Watts, D. J. and Ashworth, J. M. (1970). Metabolism of the cellular slime mould *Dictyostelium discoideum*. *Biochem. J*. **119**, 175-182.

Weissbach, L., Settleman, J., Kalady, M. F., Snijders, A. J., Murthy, A. E., Yan, Y.-X. and Bernards, A. (1994). Identification of a human RasGAP-related protein containing calmodulin-binding motifs. *J. Biol. Chem*. **269**, 20517-20521.

Westphal, M., Jungbluth, A., Heidecker, M., Mühlbauer, B., Heizer, C., Schwartz, J.-M., Mariott, G. and Gerisch, G. (1997). Microfilament dynamics during cell movement and chemotaxis motinored using a GFP-actin fusion protein. *Curr. Biol.* 7, 176-183.

Zigmond, S. H., Joyce, M., Borleis, J., Bokoch, G. M. and Devreotes, P. N. (1997). Regulation of actin polimerization in a cell-free system by GTPγS and Cdc42. *J. Cell Biol*. **138**, 363-374.

Zheng, Y., Bagrodia, S. and Cerione, R. A. (1994). Activation of phoshoinositide 3-kinase activity by Cdc42Hs binding to p85. *J. Biol. Chem*. **269**, 18727-18730.